Study on the spectral response of fiber Bragg grating sensor under non-uniform strain distribution in structural health monitoring*

HUANG Hong-mei(黄红梅) **and YUAN Shen-fang**(袁慎芳)**

Aeronautical Science Key Laboratory for Smart Material and Structures, Nanjing University of Aeronautics & Astronautics, Nanjing 210016, China

(Received 15 November 2010)

Many theoretical studies have been developed to study the spectral response of a fiber Bragg grating (FBG) under non-uniform strain distribution along the length of FBG in recent years. However, almost no experiments were designed to obtain the evolution of the spectrum when a FBG is subjected to non-uniform strain. In this paper, the spectral responses of a FBG under non-uniform strain distributions are given and a numerical simulation based on the Runge-Kutta method is introduced to investigate the responses of the FBG under some typical non-uniform transverse strain fields, including both linear strain gradient and quadratic strain field. Experiment is carried out by using loads applied at different locations near the FBG. Good agreements between experimental results and numerical simulations are obtained.

Document code: A **Article ID:** 1673-1905(2011)02-0109-4

DOI 10.1007/s11801-011-0089-9

Fiber Bragg grating (FBG) sensors are attracting much attention as a sensing device for structural health monitoring (SHM) due to their many advantages, such as small size, light weight, high accuracy, multiplexing capability, strong anti electromagnetic capability and so on[1-3]. Hence applications of FBG sensors for strain measurement in SHM have been proposed in recent years. For example, Takeda S et al[4-7] did a series of studies and judged different damages in structural health monitoring using FBG. Mckenzie et al[8] monitored the changing strain field associated with the propagation of a crack beneath the patch by using FBG sensors. Giaccari P. et al[9] demonstrated a method for measuring non-uniform strain fields using FBG sensors.

In the conventional use of the FBG, the sensors are assumed to have uniform strains along their length. In this case the shift of the Bragg wavelength is proportional to the strain[10], and this method has been well investigated. However, strain gradients such as linear or quadratic strain gradient can not be avoided in SHM. So far, some theoretical works [11-16] have been done based on transmission matrix method, but no experimental verification has been reported. Therefore, it is extremely important to investigate the spectral response of the FBG under non-uniform strain field for its application in engineering.

In this paper, we introduce a theoretical model and analyze the spectral response of the FBG in non-uniform strain fields by Runge-Kutta method. We also simulate the reflection spectra of FBG under the above-mentioned typical non-uniform strain fields. The theoretical predictions of the grating response agree well with the experimental results given.

Here we assume that the result is a perturbation to the effective refractive index n_{eff} of the guided mode(s) of interest, described by[17]

$$\delta n_{\text{eff}}(z) = \overline{\delta n_{\text{eff}}}(z)\left\{1 + v\cos\left[\frac{2\pi}{\Lambda}z + \phi(z)\right]\right\}, \tag{1}$$

where $\overline{\delta n_{\text{eff}}}(z)$is the "dc" index change spatially averaged over a grating period, v is the fringe visibility of the index change, Λ is the grating period, and $\phi(z)$ describes the grating chirp, which may be caused by fabrication or a non-uniform strain field. In this paper, the chirp is caused by a non-uniform strain field. If this factor is attributed to the period parameters, the refractive index modulation can be written as

* This work has been supported by the National High Technology Research and Development Program of China (No.2007AA03Z117), and the Key Program of National Natural Science Foundation of China (No.50830201).

** E-mail: ysf@nuaa.edu.cn

$$\delta n_{\text{eff}}(z) = \overline{\delta n_{\text{eff}}}(z)\left\{1 + v\cos\left[\frac{2\pi}{\Lambda(z)}z\right]\right\}, \tag{2}$$

where $\Lambda(z)$ is the effective period of FBG when it is subjected to a non-uniform strain.

When the fiber Bragg grating is subjected to a non-uniform strain along its length, its effective refractive index and period will be changed, so the effective period of FBG can be described by

$$\Lambda(z) = \Lambda_0[1+(1\text{-}pe)\varepsilon(z)], \tag{3}$$

where Λ_0 is the nominal period of FBG, and pe is elasto-optical coefficient of the optical fiber, whose value is 0.26. From Eqs.(1)−(3), the grating chirp $\phi(z)$ can be written as

$$\phi(z) = -\frac{2\pi z}{\Lambda_0}\left[\frac{(1-pe)\varepsilon(z)}{1+(1-pe)\varepsilon(z)}\right]. \tag{4}$$

According to the weakly guiding condition and the coupled-mode theory, we can obtain the following differential equations

$$\frac{\mathrm{d}R}{\mathrm{d}z} = \mathrm{i}\hat{\sigma}R(z) + \mathrm{i}\kappa S(z), \tag{5}$$

$$\frac{\mathrm{d}S}{\mathrm{d}z} = -\mathrm{i}\hat{\sigma}S(z) - \mathrm{i}\kappa R(z), \tag{6}$$

where R and S are the amplitudes of the forward-propagating mode and the backward-propagating mode, respectively. In these equations, $\hat{\sigma}$ is the general "dc" self-coupling coefficient and κ is the the "AC" coupling coefficient defined as

$$\hat{\sigma} = \frac{2\pi}{\lambda}\overline{\delta n_{\text{eff}}} + 2\pi n_{\text{eff}}\left(\frac{1}{\lambda} - \frac{1}{\lambda_{\text{D}}}\right) - \frac{1}{2}\frac{\mathrm{d}\phi}{\mathrm{d}z}, \tag{7}$$

$$\kappa = \frac{\pi}{\lambda}v\overline{\delta n_{\text{eff}}}. \tag{8}$$

In Eq.(7), $\lambda_{\text{D}} = 2n_{\text{eff}}\Lambda_0$ is the designed wavelength which will be changed when the FBG is subjected to various strain conditions. The reflection coefficient of the FBG is defined as

$$\rho(z) = S(z)\ /\ R(z). \tag{9}$$

By substituting Eq.(9) into Eq.(5), we can obtain the following differential equation

$$\frac{\mathrm{d}\rho(z)}{\mathrm{d}z} = -\mathrm{i}\kappa - 2\mathrm{i}\hat{\sigma}\rho(z) - \mathrm{i}k\rho^2(z). \tag{10}$$

The length of the grating is assumed to be L (L=10 mm), so the limit of the grating is defined as $-L/2 \leqslant z \leqslant L/2$. While the boundary conditions of FBG are $R(-L/2)=1$ and $S(L/2)=0$[18]. Researches have used transmission matrix method to solve Eq.(10) before. In this paper, according to Eqs.(4), (7) and (8), we solve it by Runge-Kutta method. Thus the grating's reflectivity $r = |\rho|^2$ can be obtained when the FBG is subjected to non-uniform strain.

Based on the theoretical model for predicting the spectral response of FBG together with Eq.(10), we can calculate the reflective spectra of FBG under non-uniform strain fields by MATLAB. Assume that the original Bragg wavelength, the effective refractive index, the average index, the length, Young's modulus, Poisson's coefficient, and the elasto-optical coefficients p_{11} and p_{12} of the FBG are 1550 nm, 1.45, 2×10^{-4}, 10 mm, 74.5 GPa, 0.17, 0.113 and 0.252, respectively. To demonstrate the simulated spectra of FBG subjected to different strain fields, three classical strain fields are discussed as follows.

(1) Uniform strain: $\varepsilon_0(z) = C$

Fig.1 shows the reflectivity of the grating under a uniform strain of C. It is observed that in case of C=0, that is, the stain on the FBG is 0, there is only one main peak in the reflective spectrum. In addition, the Bragg wavelength shifts to left with decreasing the value of C.

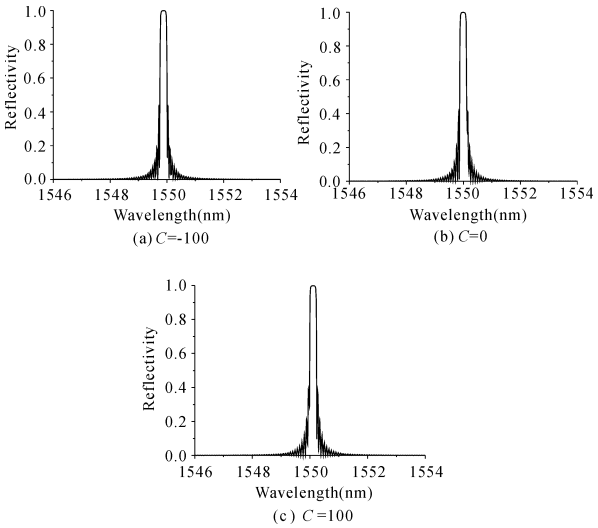

Fig.1 Reflectivity of the grating against wavelength under a uniform strain

(2) Linear strain gradient: $\varepsilon_0(z) = az$

To analyze the effect of various strain values with different strain gradients on the reflective spectrum, we consider three cases for a value, i.e., a=1, 2, 4. Note that a is the slope of the linear strain gradient. As shown in Fig.2, it is obvious that the spectrum width is broadened and the reflectivity of

the FBG is decreased with increasing the value of a. Also an obvious oscillation phenomenon is observed in the reflective spectrum.

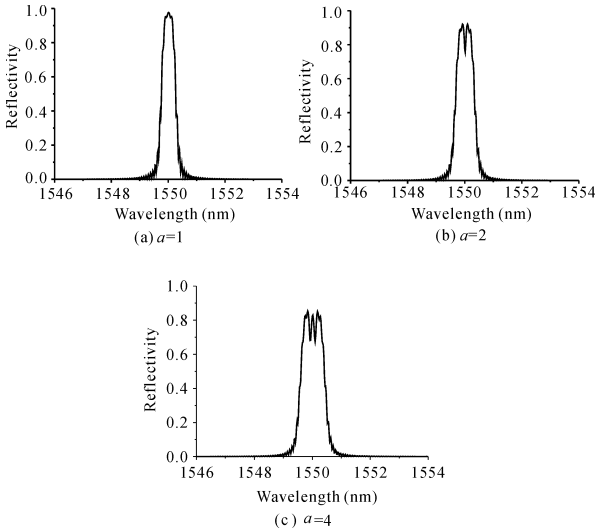

Fig.2 Reflective spectrum of the FBG under linear strain gradient

(3) Quadratic strain field: $\varepsilon_0(z) = bz^2$

Three different quadratic strain fields along the FBG are assumed to be $\varepsilon_0(z) = bz^2$ by setting b as 1, 2 and 4 (Fig.3). The shape of reflective spectrum is no longer keeping an independent peak and multiple peaks can be seen beside the main peak when the FBG is subjected to quadratic strain fields, that is, the oscillation phenomenon occurs. But the Bragg wavelength is not changed, and the value is almost equal to 1550 nm. Simultaneously, the number of peaks beside the main peak is growing and the spectrum width of the FBG is broadened with increasing the value of b.

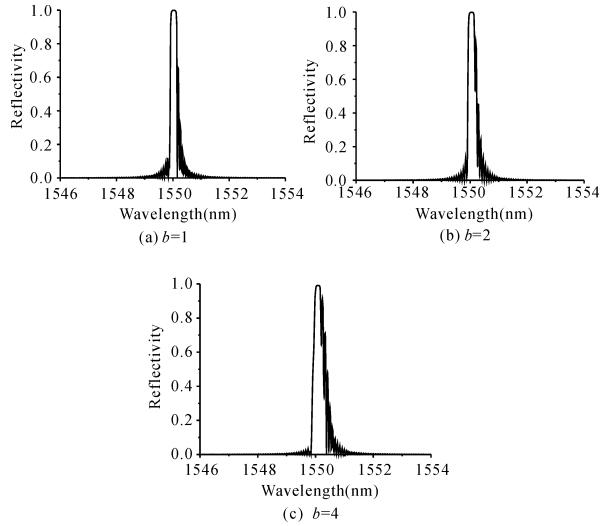

Fig.3 Reflective spectrum of the FBG under quadratic strain field

The results of the above simulations with different strain fields demonstrate the relationships between the shape, reflectivity, shift of the Bragg wavelength of the reflective spectrum and the strain distribution along the grating. It can be concluded that the distortion of the reflective spectrum becomes more obvious when the grating is subjected to higher strain gradient. Also, the shift of the Bragg wavelength is linearly related to the constant of the strain value along the grating.

An experiment is carried out to investigate the spectral response of FBG under non-uniform strain fields, and the setup is shown in Fig.4(a). The light from the broadband light source (BBS) is coupled to the FBG which has an unstrained Bragg wavelength of 1550 nm through a 3 dB coupler. The reflected light from the FBG is sent back to the optical spectrum analyzer (OSA, AQ6317 by Ando Electric Co., Ltd). The loading equipment is shown in Fig.4(b), where the bottom loading area is an aluminum plate, whose Young's modulus and Poisson's coefficient are 72.4 GPa and 0.32, respectively, and its dimension is 980 mm×580 mm×2 mm.

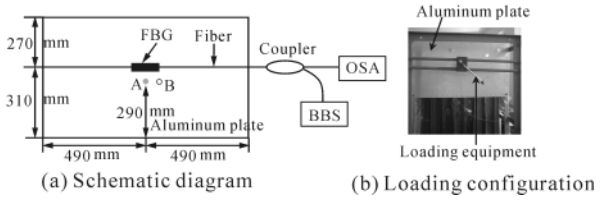

Fig.4 Experimental setup

The applied load at the location of A or B is shown in Fig.4(a). In the experiment, the applied load on the aluminum plate is 200 N. The experimental results are displayed and recorded with OSA, as presented in Fig.5.

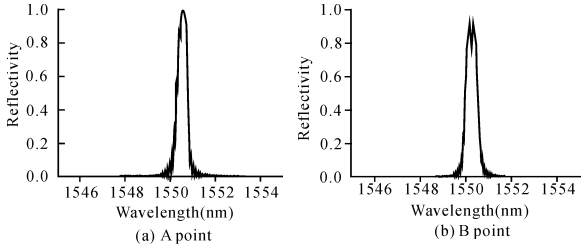

Fig.5 Reflective spectrum measured by experiment at different loading locations

In order to verify whether the experimental results coincide with the theoretical ones, a finite element model is established by ANSYS. In this step, there is no FBG in the model, but strain distribution function along the length of

FBG can be obtained. $\varepsilon(z) = -0.6\,z^2 + 101.9$ and $\varepsilon(z) = 2.87\,z + 87.5$ are strain functions when the load is applied at A and B, respectively. Then combined with Eqs.(7), (8) and (10), the reflective spectra at different loading locations of A and B can be predicted by Runge-Kutta method, as shown in Fig.6. From Fig.5 and Fig.6, we can see that the experimental results correspond well to the theoretical predictions.

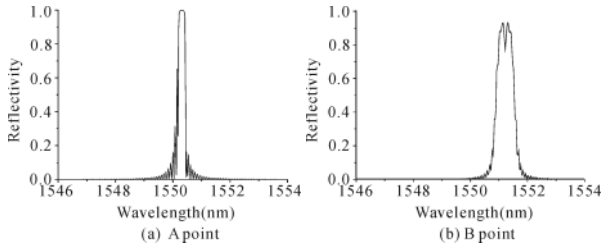

Fig.6 Calculated reflective spectrum at different loading locations

A study of spectral response of FBG under non-uniform strain distribution along the length of FBG is introduced by means of Runge-Kutta method. The proposed method is validated by applying different strain fields: linear strain gradient and quadratic strain field along the length of the fiber Bragg grating. The experiment is carried out to verify the theoretical predictions. It is important to note that this FBG sensing system can be employed for structural health monitoring during its in-service time, and we can identify the type of damages by the change of the reflective spectrum.

References

[1] BAO Jilong, Zhang Xian-min and Chen Kang-sheng, Laser Technology **24**, 174 (2000). (in Chinese)

[2] Mousumi Majumder, Tarun Kumar Gangopadhyay and Ashim Kumar Chakraborty, J. Sensors and Actuators A **147**, 150 (2008).

[3] WANG Hong-liang, WANG Lin and JIA Zhen-an, Journal of Optoelectronics • Laser **20**, 526 (2009). (in Chinese)

[4] Takeda S, Okabe Y, Yamamoto T and Takeda N, Comp. Sci. Technol. **63**, 1885 (2003).

[5] Takeda S, Minakuchi S, Okabe Y and Takeda N, Composites A **36**, 903 (2005).

[6] S Takeda, T Yamamoto, Y Okabe and N Takeda, Smart Mater. Struct. **16**, 763 (2007).

[7] Takeda S, Aoki Y, Ishikawa, Takeda N and Kikukawa, Comp. Struct. **79**, 133 (2007).

[8] McKenzie, R. Jones, I. H. Marshall and S. Galea, J. Composite Structures **50**, 405 (2000).

[9] Giaccari P, Dunkel G R, Humbert L, Botsis J, Limberger H G and Salath´e R P, J. Smart Mater. Struct. **14**, 127 (2000).

[10] Yuan Shen-fang, Structural Health Monitoring and Damage Control, Beijing, 2007. (in Chinese)

[11] WU Fei, LI Li-xin and LI Zhi-quan, Chinese Journal of Lasers **33**, 472 (2006). (in Chinese)

[12] Cai Lu-Lu, Yin Wen-Wen and Wu Fei, Acta Physica Sinica **57**, 7737 (2008). (in Chinese)

[13] YANG Guo-fu, Chinese Journal of Sensors and Actuators **20**, 1021 (2007). (in Chinese)

[14] Yiping Wang, Na Chen, Binfeng Yun, Zhuyuan Wang, Changgui Lu and Yiping Cui, Optics & Laser Technology **40**, 1037 (2008).

[15] Hang-Yin Ling, Kin-Tak Lau, Wei Jin and Kok-Cheung Chan, Optics Communications **270**, 25 (2007).

[16] P. Torres and L. C. G. Valentec, Optics Communications **208**, 285 (2002).

[17] Turan Erdogan, J. Lightwave Technology **15**, 1277 (1997).